Physics of Seismo-electromagnetic Phenomena

H.G. Silva[1] and M. Bezzeghoud[1,2]

[1]*Geophysics Centre of Évora, University of Évora, Portugal*
[2]*Department of Physics, University of Évora, Portugal*

Outline

- Seismic Precursors
- Seismo-Electromagnetic Phenomena (SEM)
- Field Observations
  - Project
  - Atmospheric Electric Field (Sousel EQ)
- Laboratorial Experiments
  - Electric Transport in Granitic Rocks
- Theoretical Model
  - Piezoelectric Effect During Crack Propagation
- Publications

Seismic precursors

Journal of Zoology ZSL
Journal of Zoology. Print ISSN 0952-8369

Predicting the unpredictable; evidence of pre-seismic anticipatory behaviour in the common toad

R. A. Grant[1] & T. Halliday[2]
1 Department of Life Sciences, The Open University, Milton Keynes, UK
2 Oxford, UK

Nat. Hazards Earth Syst. Sci., 9, 1221–1226, 2009
www.nat-hazards-earth-syst-sci.net/9/1221/2009/

Natural Hazards and Earth System Sciences

Specific variations of the atmospheric electric field potential gradient as a possible precursor of Caucasus earthquakes

N. Kachakhidze[1], M. Kachakhidze[1], Z. Kereselidze[2], and G. Ramishvili[3]
…, I. Chavchavadze av., 0128, Tbilisi, Georgia
…ysics, 1, Alexidze str., 0183, Tbilisi, Georgia
…ity, National Astrophysical Observatory, 2, Kazbegi av., 0160, Tbilisi, Georgia

Contents lists available at ScienceDirect
Physics and Chemistry of the Earth
journal homepage: www.elsevier.com/locate/pce
ELSEVIER

Preseismic changes in atmospheric radon concentration and crustal strain

Yumi Yasuoka[a,*], Yusuke Kawada[b,c], Hiroyuki Nagahama[b], Yasutaka Omori[b], Tetsuo Ishikawa[d], Shinji Tokonami[d], Masaki Shinogi[a]
[a] Institute of Radioisotope Research, Kobe Pharmaceutical University, Kobe 658-8558, Japan
[b] Department of Geoenvironmental Sciences, Graduate School of Science, Tohoku University, Sendai 980-8578, Japan
[c] School of GeoSciences, University of Edinburgh, Edinburgh EH9 3JW, UK
[d] National Institute of Radiological Sciences, Chiba 263-8555, Japan

GEOPHYSICAL RESEARCH LETTERS, VOL. 17, NO. 9, PAGES 1465-1468, AUGUST 1990

LOW-FREQUENCY MAGNETIC FIELD MEASUREMENTS NEAR THE EPICENTER OF THE M_S 7.1 LOMA PRIETA EARTHQUAKE

A. C. Fraser-Smith, A. Bernardi[1], P. R. McGill,
M. E. Ladd, R. A. Helliwell, and O. G. Villard, Jr.
STAR Laboratory, Stanford University

SEM Phenomena

- Anomalous electrical signals
- Abnormal ultra-low frequency EM emissions
- Anomalies in very-low and low frequency radio transmissions
- Variation of the total electron content (TEC) in the ionosphere
- Atypical IR emissions

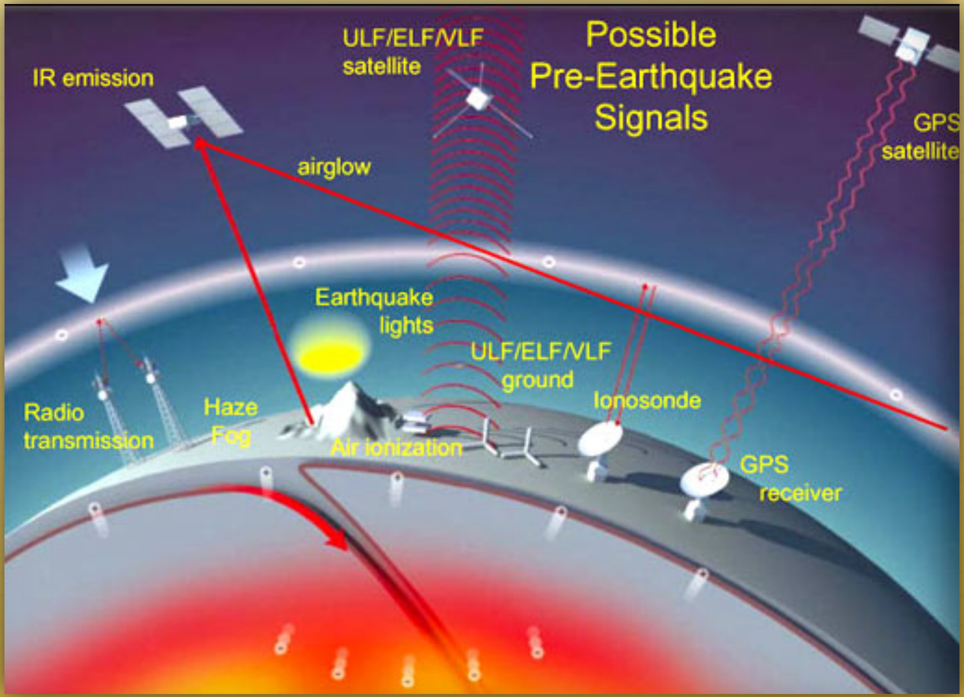

Extrated from: http://www.quakefinder.com/

Field Observations

with

C. Serrano, A.H. Reis, R.N. Rosa, J.F. Borges, B. Caldeira e M. Tlemçani, A. Araújo, and P.F. Biagi*

**Department of Physics, University of Bari, Italy*

Project

Atmospheric Electric Field Sensor

Radio Receiver for VLF/LF signals

Magnetometers for ultra-low frequencies (planned)

Atmospheric Radon Meter (installation)

Sousel Earthquake

The EQ occurred March 27, 2010 in Sousel (Alentejo) with a depth of 15 km and magnitude of $M_L = 4.1$ (IM).

The electric field sensor was placed ~52 km from the EQ epicentre and within its preparation zone.

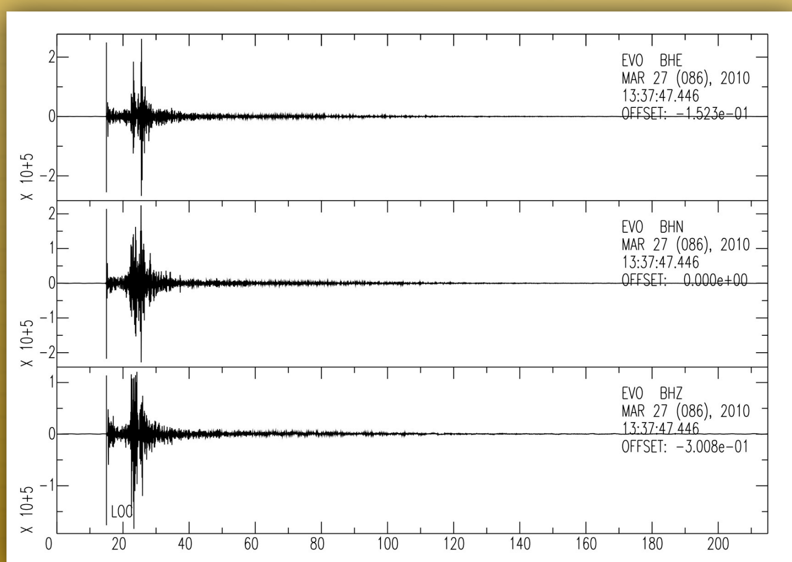

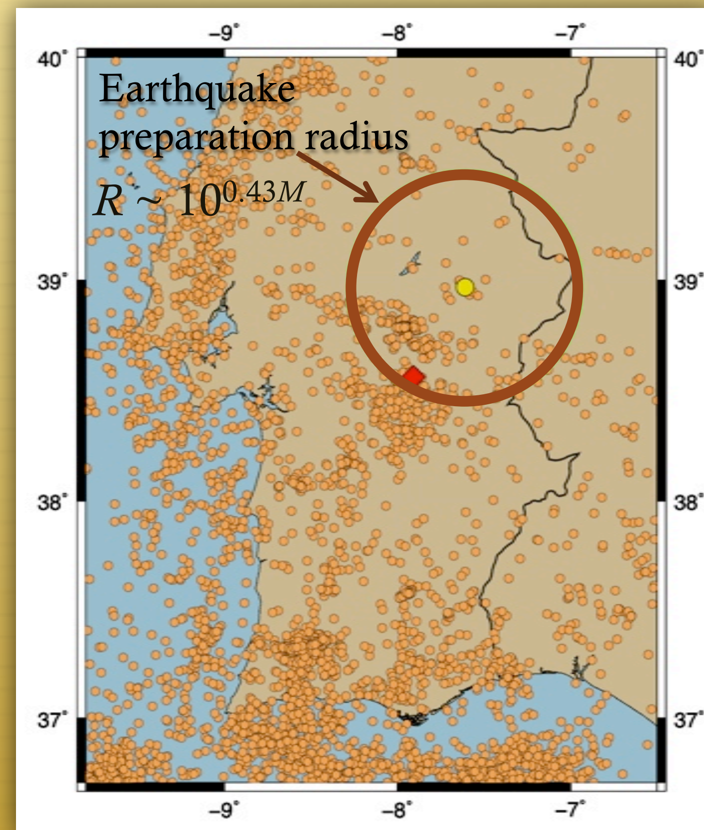

Atmospheric electric field

The electric field sensor is a JCI 131 installed at the University of Évora. This equipment is in operation since February 2005 to date.

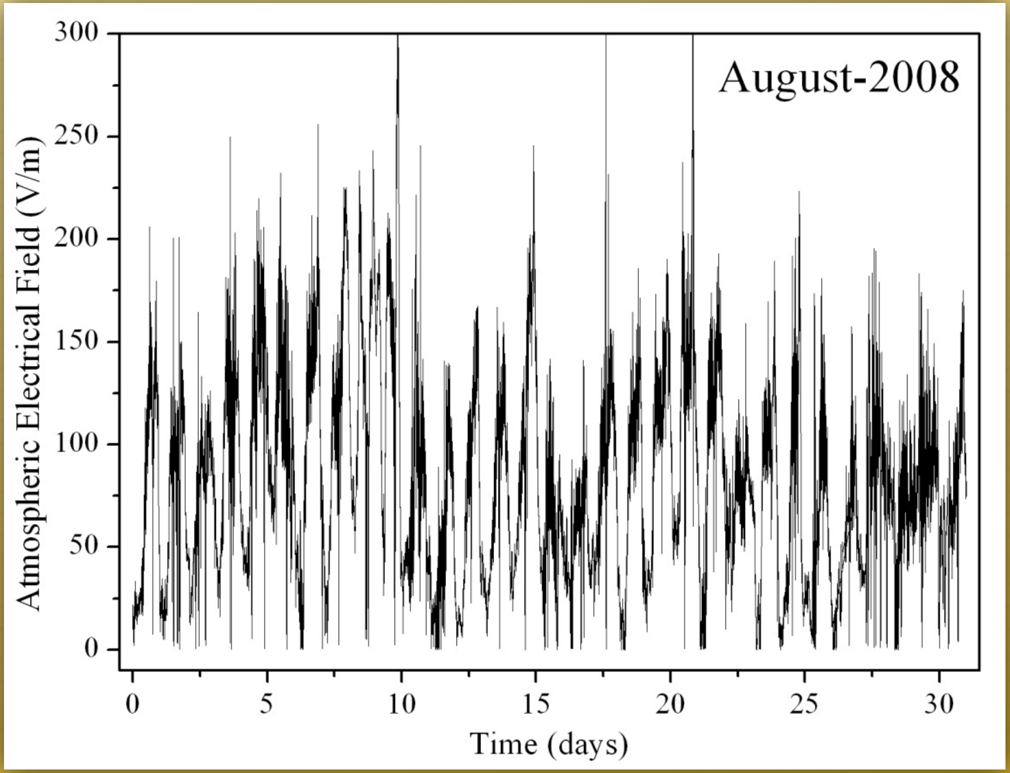

Usual atmospheric electric field.

In this study we concentrate on the period from January 2007 until December 2010.

Atmospheric electric field

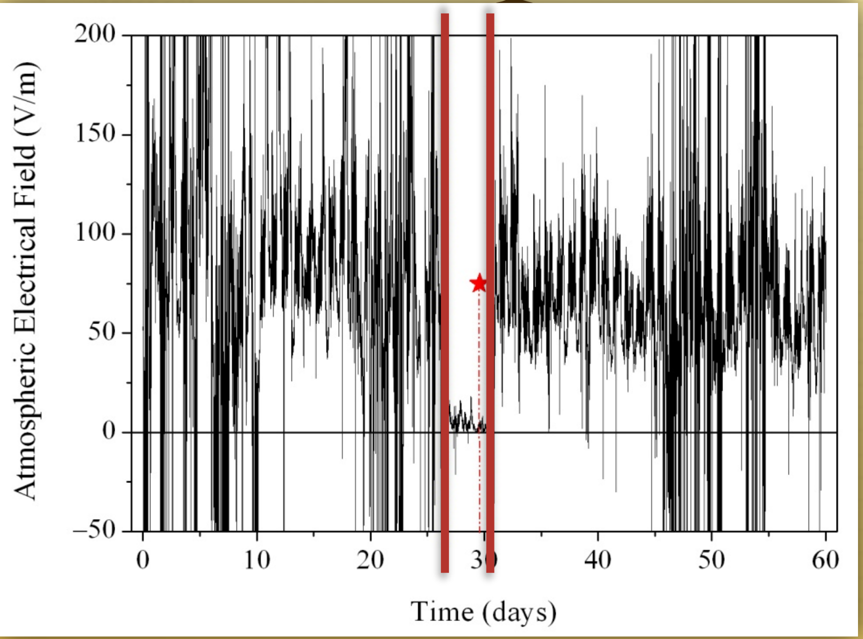

Atmospheric electric field: the EQ is marked with a red star.

No human disturbance or malfunction of the equipment was found

Weather conditions during the earthquake: the blue lines indicate the duration of the decrease of atmospheric electric field.

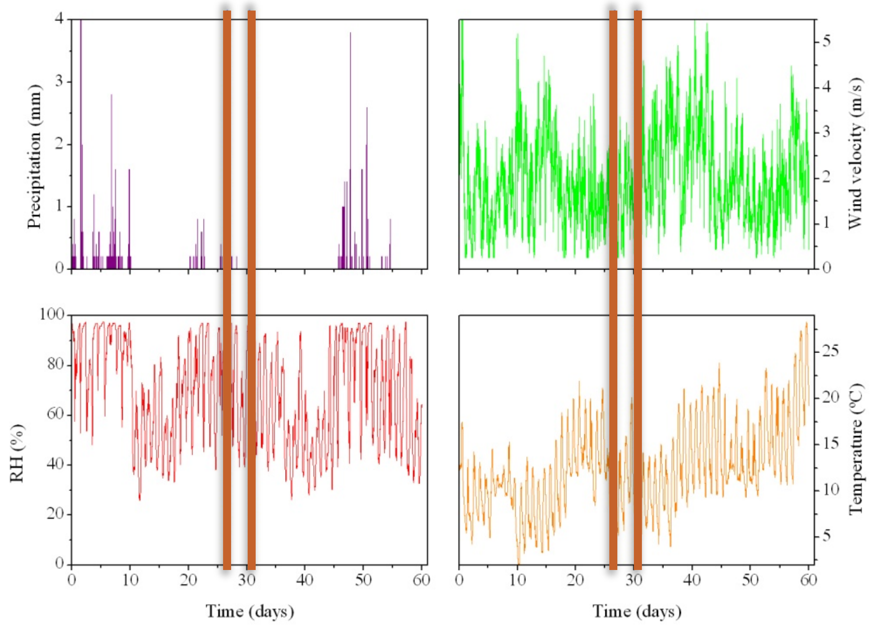

The weather conditions fit nearly fair-weather

Atmospheric electric field

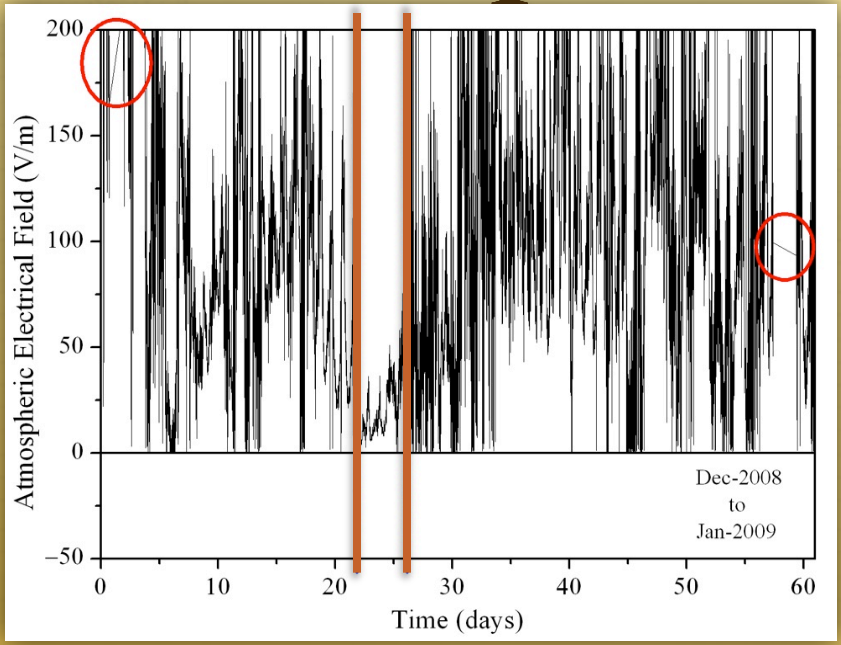

For this event no significant seismic activity occurred in the region

Atmospheric electric field: in which there was a decrease in the atmospheric electric field

Weather conditions during the referred period

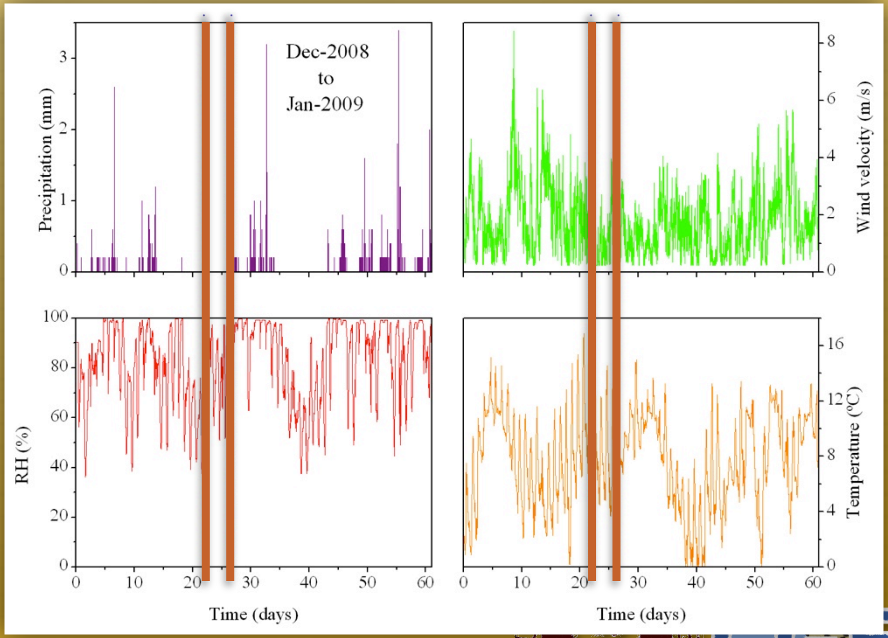

The weather conditions were similar to the Sousel earthquake

Atmospheric electric field

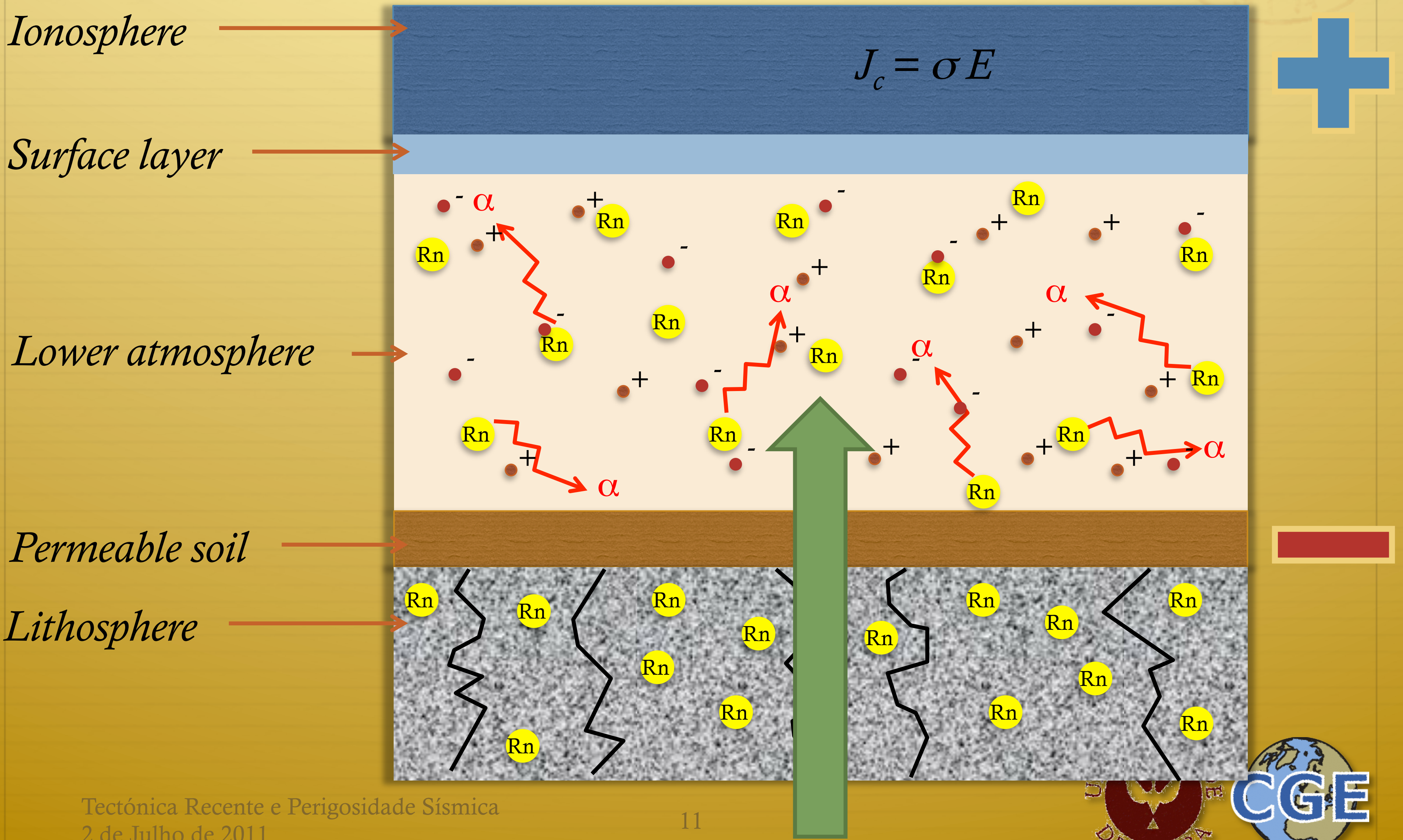

AEF: sum-up

- This study provides the first clear evidence of a significant reduction of the vertical component of atmospheric electric field in the preparatory phase of a seismic event.
- These observations support the idea that the radon emanations are the mechanism behind this decrease.
- Additional work is needed to confirm this hypothesis, in particular, the systematic measurement of radon levels is essential.
- The installation of new atmospheric electric field sensors, magnetometers, and radon detectors in seismic regions (evaluation of multiple parameters) is another step in the project.

Laboratorial Experiments

with

M.P.F. Graça*, J. H. Monteiro*, R.N. Rosa, S. K. Mendiratta*, M. Tlemçani, P. Moita

**Physics Department, and I3N, University of Aveiro, Portugal*

Impedance spectroscopy

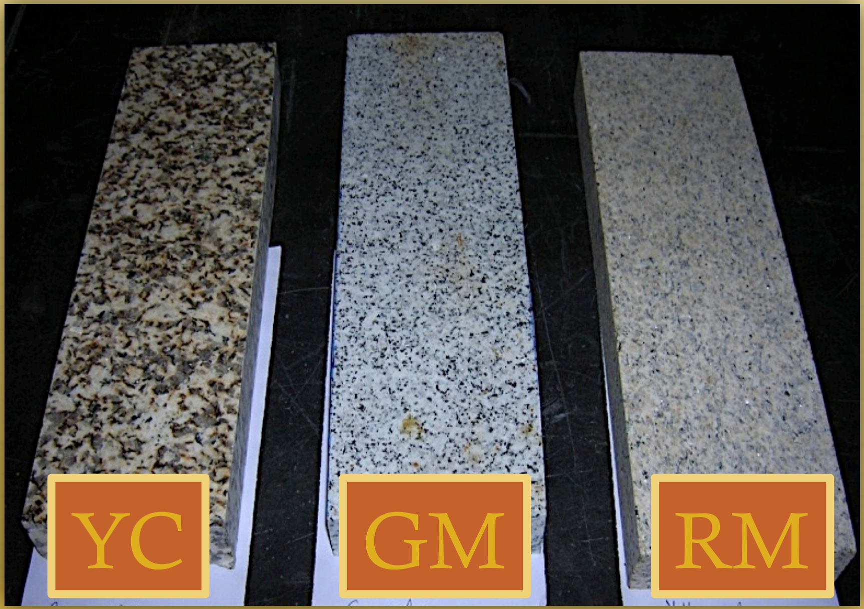

YC is a porphiritic coarse grained biotitic-muscovitic granite, yellow coloured and characterized by an abundance of large feldspar usually showing poorly defined shapes.

RM is a granite with a homogeneous medium grained matrix (occasionally coarser grained quartz) and light rosy coloured determined by the tonality of the feldspar crystals that stand out from a greyish matrix.

GM is a granodiorite grey coloured and medium grained rock with homogeneous appearance. Dark minerals is mainly biotite.

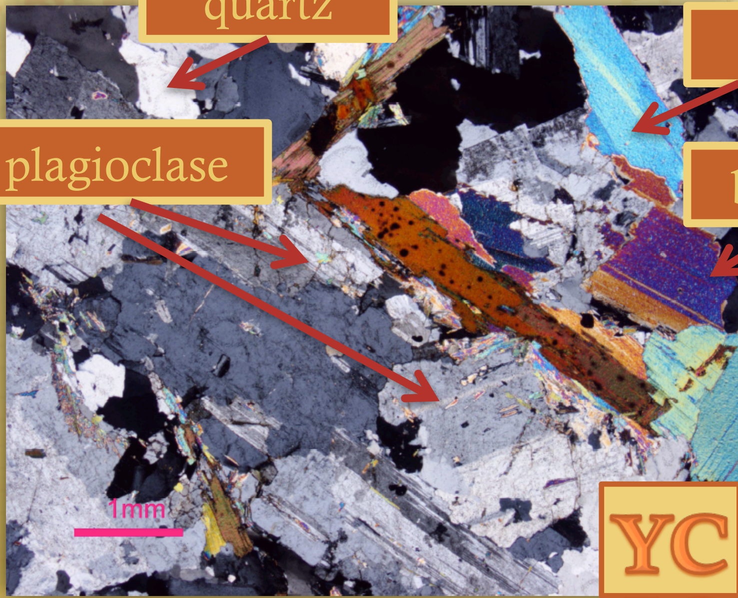
quartz
muscovite
plagioclase
biotite
1mm
YC

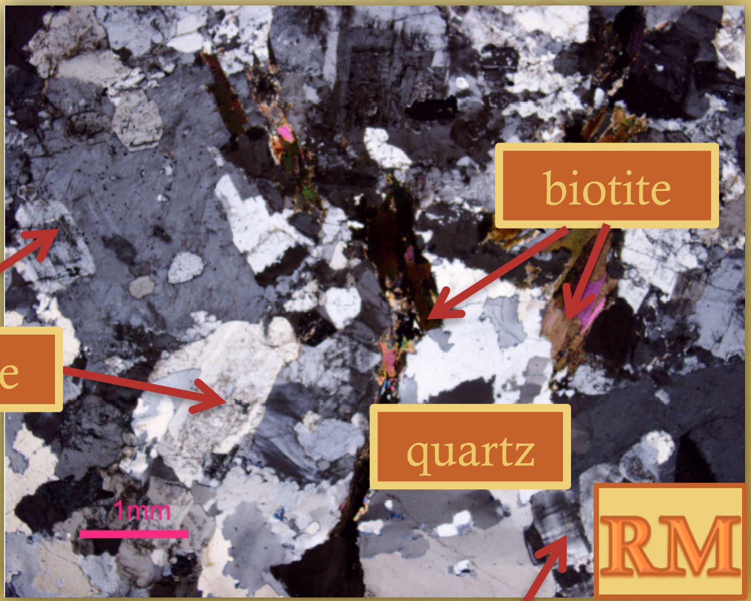
biotite
plagioclase
quartz
1mm
RM
Alkaline feldspar


Alkaline feldspar
quartz
biotite
plagioclase
1mm
GM

Impedance spectroscopy

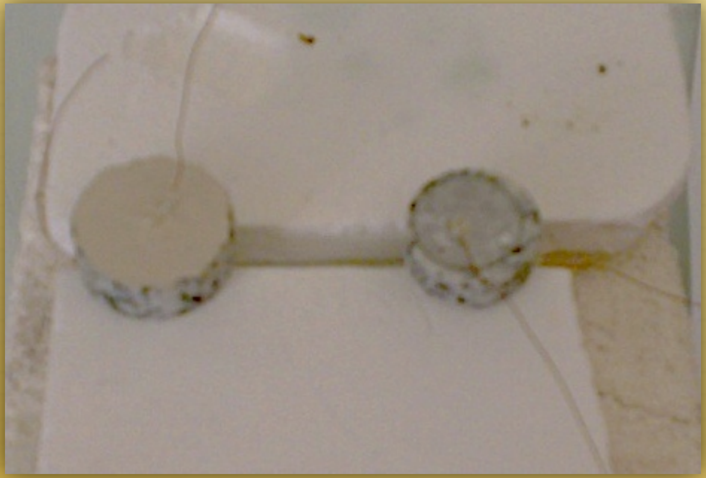

Circular samples with approximately 24 mm diameter and 2-4 mm in thicknesses were prepared. Once cut and carefully polished (with a 15 μm polishing disc) the samples here heated from room-temperature (RT) up to ~400 K and after cooled down again.

Circular electrodes with a diameter of 20 mm were then established using silver conductive paint (in the future, new contacts will be tested). The samples were submitted again to a heat treatment at ~400 K to evaporate the silver paint solvent.

Impedance spectroscopy

Impedance spectroscopy was done with $V_{AC} = 1\ V$ test signal in the frequency range of 40 Hz to 1 MHz at stabilized temperatures ranging from 100 K to 360 K. It was used an Agilent 4294A Precision Impedance Analyzer.

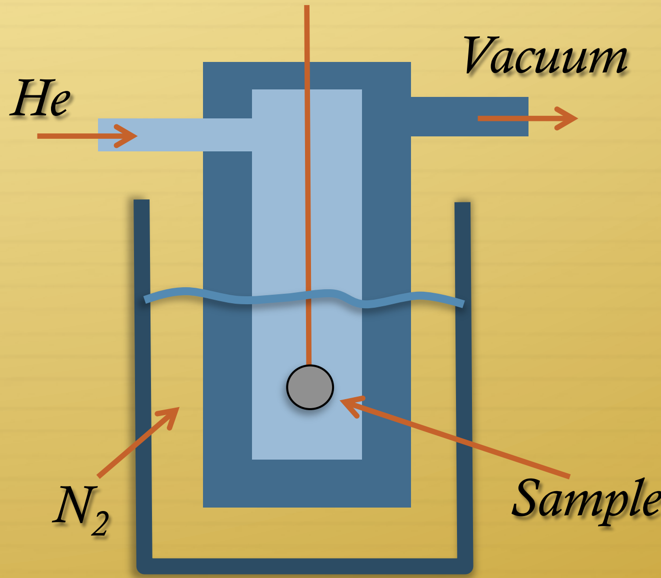

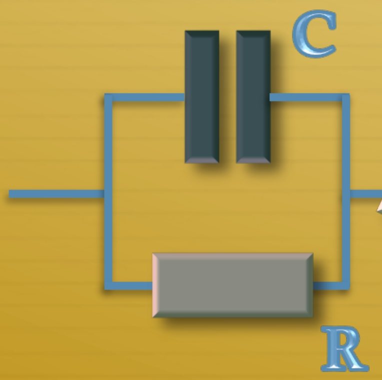

$$\varepsilon^*(\omega) = \varepsilon'(\omega) + i\varepsilon''(\omega)$$

$$K'(\omega) = \frac{\varepsilon'}{\varepsilon_0} = \frac{d}{\varepsilon_0 A}\frac{\sin[\phi(\omega)]}{|Z(\omega)|\omega}$$

$$K''(\omega) = \frac{\varepsilon''}{\varepsilon_0} = \frac{d}{\varepsilon_0 A}\frac{\cos[\phi(\omega)]}{|Z(\omega)|\omega}$$

Impedance spectroscopy

Impedance spectra at different temperatures: a) Real part of the dielectric constant; b) Imaginary part of the dielectric constant.

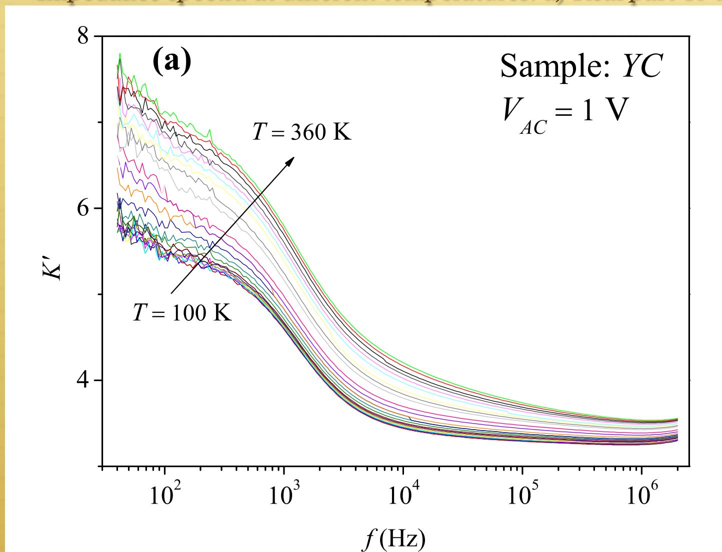

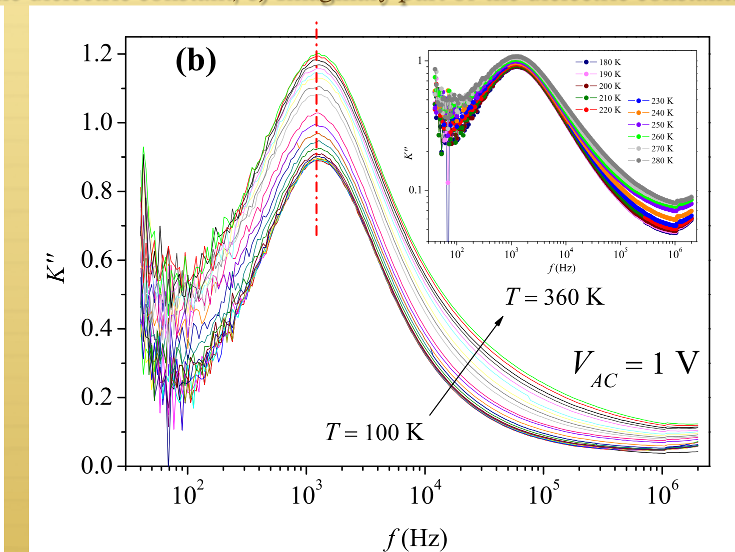

Real and Imaginary part of ε as a function of temperature: a) *f* = 100 Hz; b) *f* = 1027 Hz; c) *f* = 10 520 Hz; d) comparison.

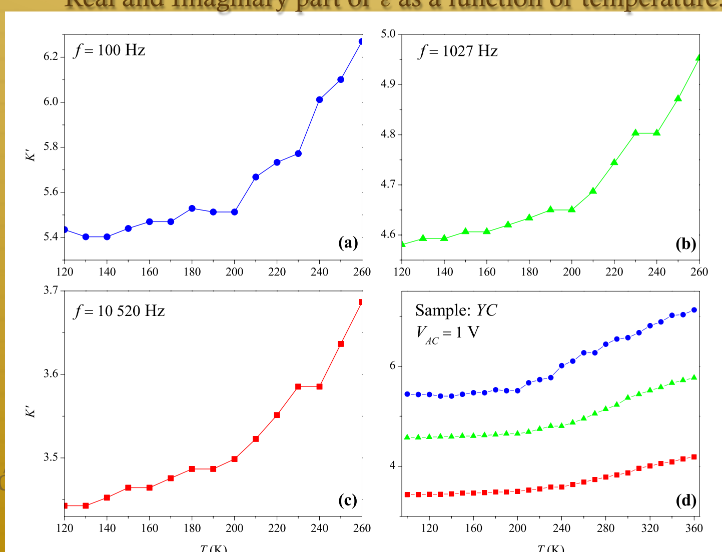

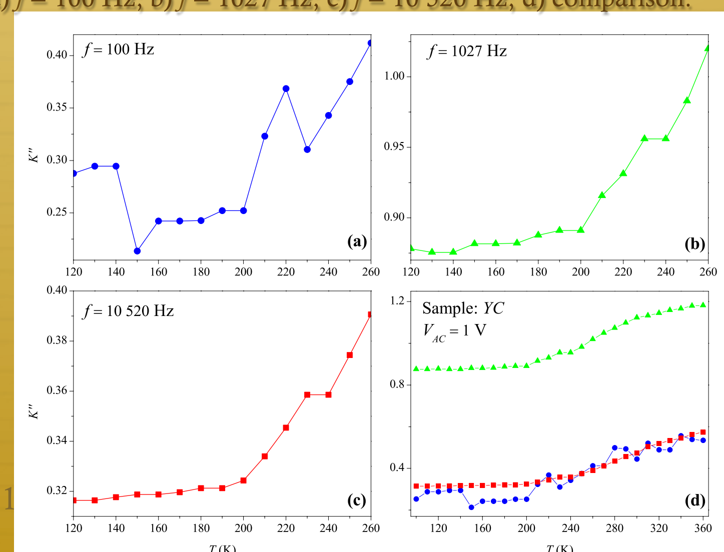

Tect
de

YC

Impedance spectroscopy

Impedance spectra at different temperatures: a) Real part of the dielectric constant; b) Imaginary part of the dielectric constant.

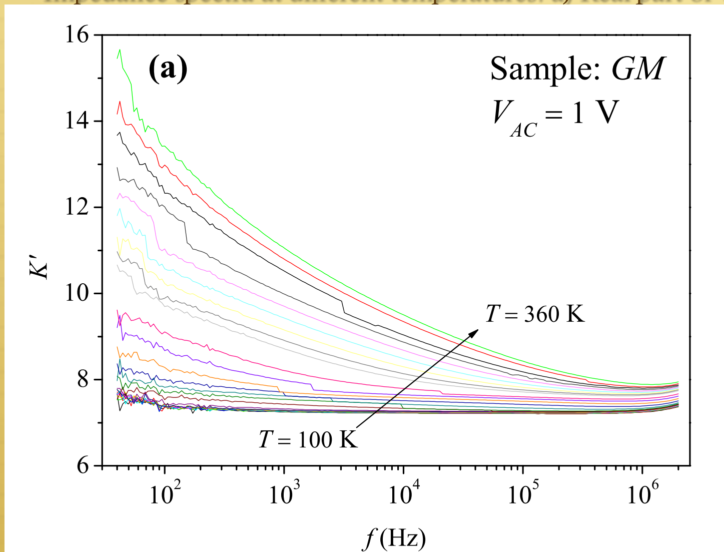

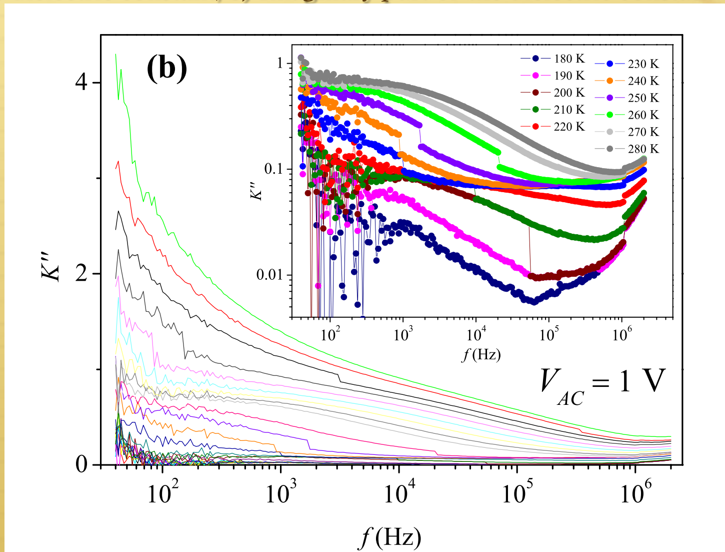

Real and Imaginary part of ε as a function of temperature: a) f = 100 Hz; b) f = 1027 Hz; c) f = 10 520 Hz; d) comparison.

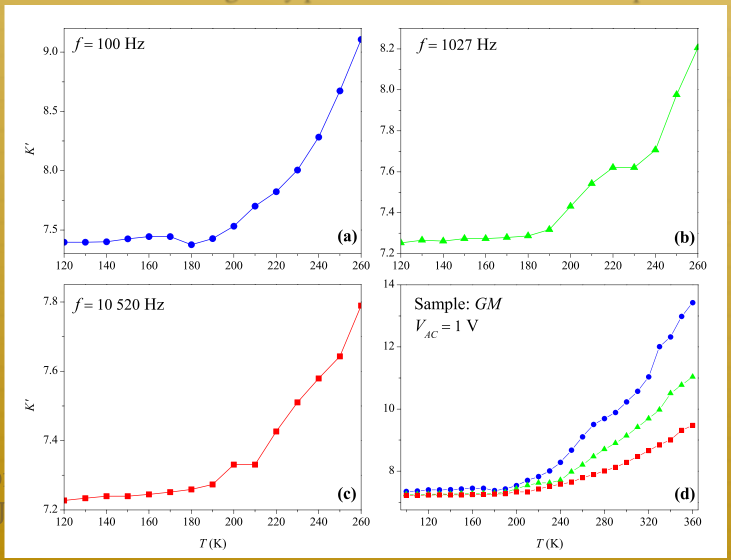

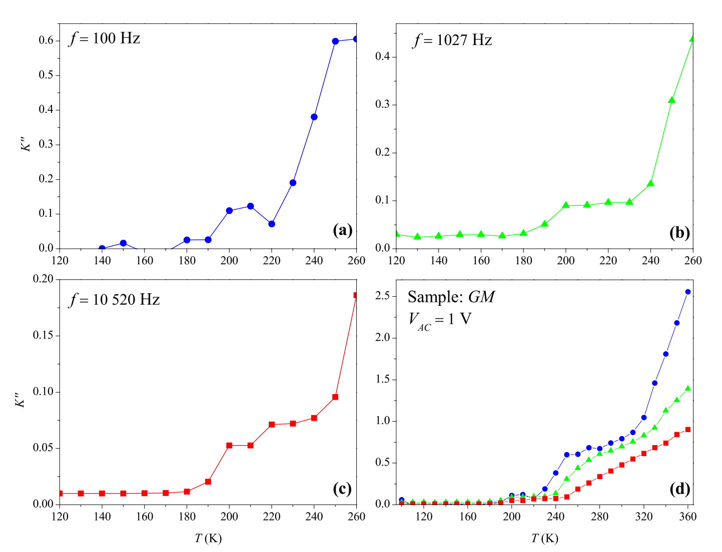

Impedance spectroscopy

Impedance spectra at different temperatures: a) Real part of the dielectric constant; b) Imaginary part of the dielectric constant.

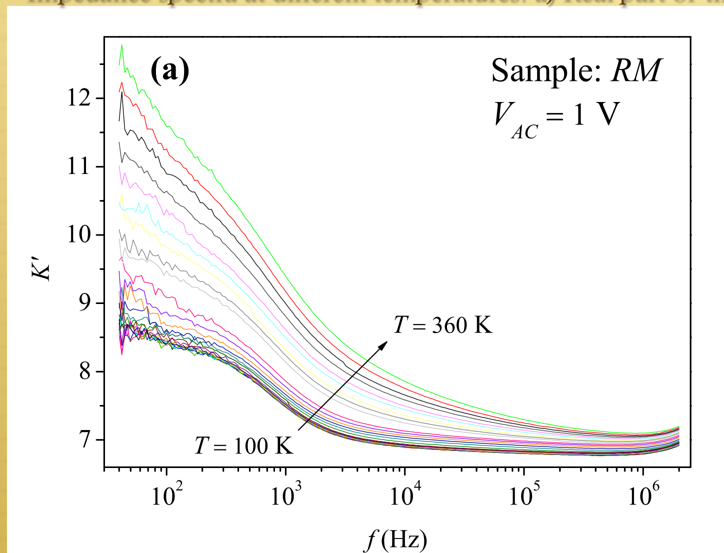

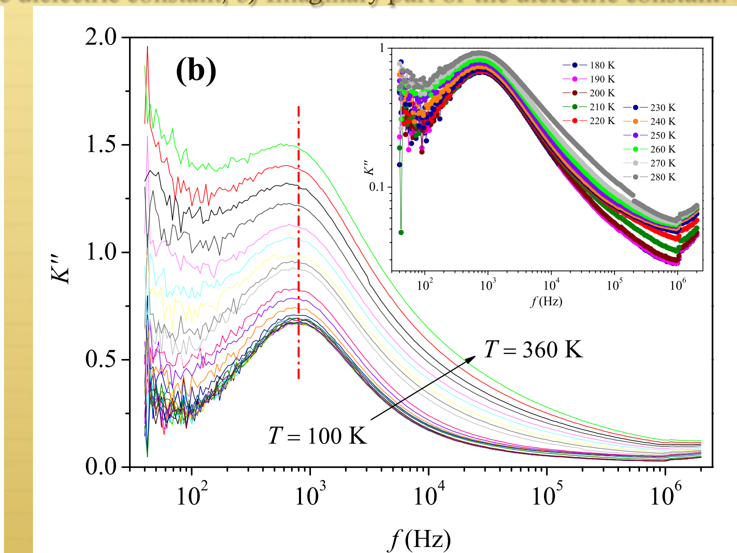

Real and Imaginary part of ε as a function of temperature: a) *f* = 100 Hz; b) *f* = 1027 Hz; c) *f* = 10 520 Hz; d) comparison.

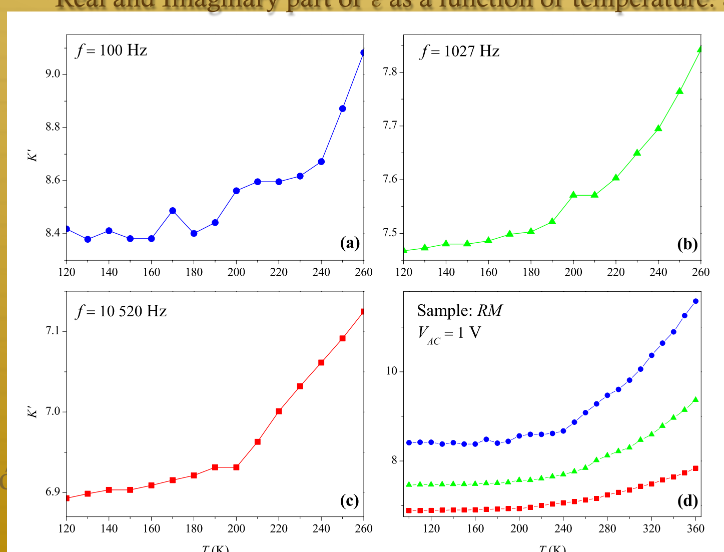

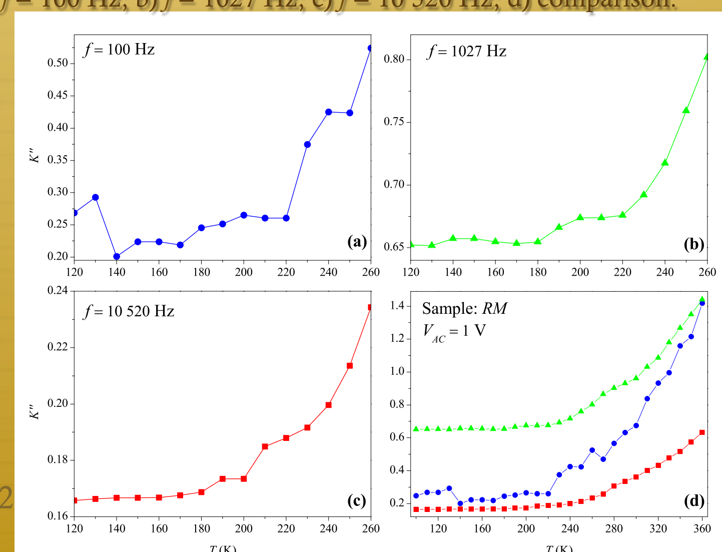

IS: sum-up

- An anomaly in the dielectric behaviour near $T \sim 220$ K is found.
- This temperature is typical of the super-cooled phase transition of strongly confined water affecting electronic devises.
- Samples *YC* and *RM* show a relaxation process taking place at $f \sim 10^3$ Hz readily evidenced in the K″ curves here a significant peak appears at this frequency that does not change with temperature.
- Our final objective is to Investigate possible mechanisms of charge creation in different crust materials and conditions (pressure and temperature).

Theoretical Model

with

Pedro M. Areias*, José E. Garção*, Nicolas Van Goethem§

**Physics Department, University of Évora, Portugal*
§Mathematics Department, Faculty of Sciences, University of Lisbon, Portugal

Piezoelectric effect

Mass conservation

$$\frac{\partial (J\rho)}{\partial t} = 0 \qquad \text{with} \qquad J = \det \boldsymbol{F}$$

Cauchy equation of motion and Cauchy lemma

$$\nabla \cdot \boldsymbol{\sigma} = \rho \frac{\mathrm{D}\dot{\boldsymbol{u}}}{\mathrm{D}t}$$

$$\boldsymbol{n}^T \boldsymbol{\sigma} = \boldsymbol{t}$$

Piezoelectric effect

Maxwell's equations for insulators $\rho_{\text{free}} = 0$ and $\boldsymbol{j}_{\text{free}} = \boldsymbol{0}$.

$$\begin{aligned} \nabla \times \boldsymbol{h} + \dot{\boldsymbol{d}} &= 0 \\ \nabla \cdot \boldsymbol{b} &= 0 \\ \nabla \times \boldsymbol{e} + \dot{\boldsymbol{b}} &= 0 \\ \nabla \cdot \boldsymbol{d} &= 0 \end{aligned}$$

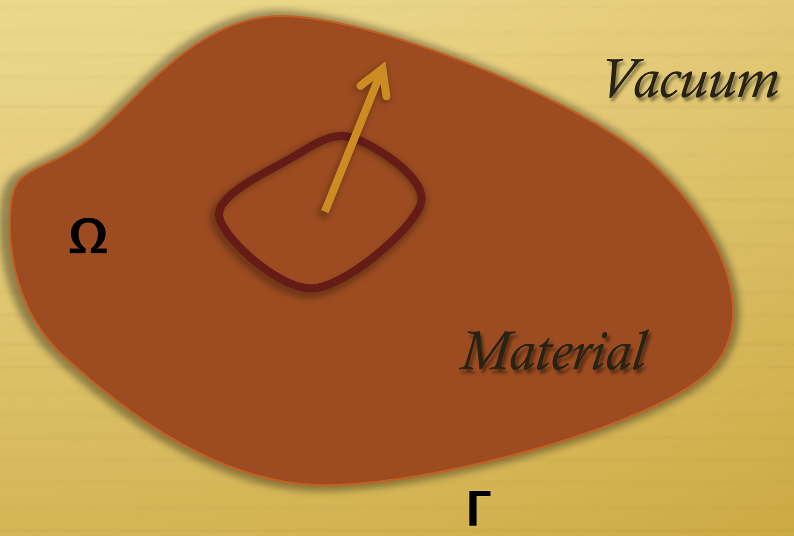

With boundary conditions

$$\boldsymbol{n} \cdot [[\boldsymbol{b}]] = \boldsymbol{0} \qquad \boldsymbol{n} \times [[\boldsymbol{h} - \boldsymbol{v} \times \boldsymbol{d}]] = \boldsymbol{0}$$
$$\boldsymbol{n} \cdot [[\boldsymbol{d}]] = \boldsymbol{0} \qquad \boldsymbol{n} \times [[\boldsymbol{e} + \boldsymbol{v} \times \boldsymbol{b}]] = \boldsymbol{0}$$

Piezoelectric effect

Strain tensor

$$\boldsymbol{\varepsilon} = \frac{1}{2}\left(\boldsymbol{b} - \boldsymbol{I}\right)$$

Ogdon model, N=2 *(Mooney-Rivlin material)*

Total Helmoltz free energy

Derived to generate the correct expression for the Maxwell stress tensor

$$\overline{\psi}(\boldsymbol{\varepsilon}, \boldsymbol{d}, \boldsymbol{h}) = \frac{1}{2}\left(1 - D\right)\boldsymbol{\varepsilon}^T : \mathcal{C} : \boldsymbol{\varepsilon} + \frac{1}{2}\mu \boldsymbol{h}^T(\boldsymbol{I} + 2\boldsymbol{\varepsilon})\boldsymbol{h} + \frac{1}{2\epsilon}\boldsymbol{d}^T(\boldsymbol{I} + 2\boldsymbol{\varepsilon})\boldsymbol{d} - \frac{1}{2}\left(\frac{1}{\epsilon}\boldsymbol{d}\cdot\boldsymbol{d} + \mu\boldsymbol{h}\cdot\boldsymbol{h}\right)\mathrm{tr}[\boldsymbol{\varepsilon}] + \boldsymbol{d}\cdot(\mathcal{I} : \boldsymbol{\varepsilon})$$

Deformation energy

Electromagnetic terms

Piezoelectric effect

Where D is the damage variable

Piezoelectric effect

The corresponding damage loading function

$$\varphi(\boldsymbol{\varepsilon}) = (1 - D)\varepsilon_1 - \varepsilon_{\max}$$

The following loading/unloading conditions

$$\varphi(\boldsymbol{\varepsilon}) \leq 0$$

$$\dot{D}\varphi(\boldsymbol{\varepsilon}) = 0$$

$$\dot{D} \geq 0$$

The Kirchhoff stress tensor, the electric field and the magnetic induction

$$\boldsymbol{\tau} = \frac{\partial\overline{\psi}}{\partial\boldsymbol{\varepsilon}} \qquad \boldsymbol{e} = \frac{\partial\overline{\psi}}{\partial\boldsymbol{d}} \qquad \boldsymbol{b} = \frac{\partial\overline{\psi}}{\partial\boldsymbol{h}}$$

Piezoelectric effect

The first variation of $\boldsymbol{\tau}$, $\boldsymbol{e}$ and $\boldsymbol{b}$ with respect to $\boldsymbol{\varepsilon}$, $\boldsymbol{d}$ and $\boldsymbol{h}$

$$\delta\boldsymbol{\tau} = \frac{\partial^2\overline{\psi}}{\partial\boldsymbol{\varepsilon}^2} : \delta\boldsymbol{\varepsilon} + \frac{\partial^2\overline{\psi}}{\partial\boldsymbol{\varepsilon}\partial\boldsymbol{d}} \cdot \delta\boldsymbol{d} + \frac{\partial^2\overline{\psi}}{\partial\boldsymbol{\varepsilon}\partial\boldsymbol{h}} \cdot \delta\boldsymbol{h}$$

$$\delta\boldsymbol{e} = \frac{\partial^2\overline{\psi}}{\partial\boldsymbol{d}\partial\boldsymbol{\varepsilon}} : \delta\boldsymbol{\varepsilon} + \frac{\partial^2\overline{\psi}}{\partial\boldsymbol{d}^2} \cdot \delta\boldsymbol{d} + \frac{\partial^2\overline{\psi}}{\partial\boldsymbol{d}\partial\boldsymbol{h}} \cdot \delta\boldsymbol{h}$$

$$\delta\boldsymbol{b} = \frac{\partial^2\overline{\psi}}{\partial\boldsymbol{h}\partial\boldsymbol{\varepsilon}} : \delta\boldsymbol{\varepsilon} + \frac{\partial^2\overline{\psi}}{\partial\boldsymbol{h}\partial\boldsymbol{d}} \cdot \delta\boldsymbol{d} + \frac{\partial^2\overline{\psi}}{\partial\boldsymbol{h}^2} \cdot \delta\boldsymbol{h}$$

*The third derivatives with respect $\boldsymbol{\varepsilon}$, **d** and **h** are also needed for $\boldsymbol{b}$*

Piezoelectric effect

Integrating in Ω provides the virtual work

$$\delta W = \int_{\Omega_0} \boldsymbol{\tau} : \nabla\delta\boldsymbol{u}\,\mathrm{d}\Omega_0 + \int_{\Omega_0} \dot{\boldsymbol{b}}\cdot\delta\boldsymbol{h}\,\mathrm{d}\Omega_0 - \int_{\Omega_0} (\nabla\times\delta\boldsymbol{h})\cdot\boldsymbol{e}\,\mathrm{d}\Omega_0 + \int_{\Omega_0}\left(\nabla\times\boldsymbol{h}-\dot{\boldsymbol{d}}\right)\cdot\delta\boldsymbol{d}\,\mathrm{d}\Omega_0 +$$
$$r_b\int_{\Omega_0}\nabla\cdot\boldsymbol{b}\nabla\cdot\delta\boldsymbol{b}\mathrm{d}\Omega_0 + r_d\int_{\Omega_0}\nabla\cdot\boldsymbol{d}\nabla\cdot\delta\boldsymbol{d}\mathrm{d}\Omega_0 + \int_\Gamma \delta\lambda_b^I\boldsymbol{n}\cdot[[\boldsymbol{b}]]\mathrm{d}\Gamma + \int_\Gamma\delta\lambda_d^I\boldsymbol{n}\cdot[[\boldsymbol{d}]]\mathrm{d}\Gamma +$$
$$\int_\Gamma\delta\lambda_d^{II}\boldsymbol{n}\times[[\boldsymbol{h}-\boldsymbol{v}\times\boldsymbol{d}]]\mathrm{d}\Gamma + \int_\Gamma\delta\lambda_b^{II}\boldsymbol{n}\times[[\boldsymbol{e}+\boldsymbol{v}\times\boldsymbol{b}]]\mathrm{d}\Gamma - \int_{\Gamma_t}\boldsymbol{t}\cdot\delta\boldsymbol{u}\mathrm{d}\Gamma_t + \int_\Gamma\boldsymbol{e}\times\delta\boldsymbol{h}\,\mathrm{d}\Gamma = 0$$

The second variation of W is also required for the application of Newton's method.

The backward-Euler method is used for the integration

$$\dot{\boldsymbol{b}} \cong \frac{\boldsymbol{b}_{n+1}-\boldsymbol{b}_n}{\Delta t}$$
$$\dot{\boldsymbol{d}} \cong \frac{\boldsymbol{d}_{n+1}-\boldsymbol{d}_n}{\Delta t}$$

Piezoelectric effect

The δ-variation of $\nabla(\bullet)$

$$\delta\nabla(\bullet) = \nabla\delta(\bullet) - \nabla(\bullet)\nabla\delta\boldsymbol{u}$$

Here $\bullet$ is a tensor and ∇ is a spatial gradient

The d-variation of $\nabla(\bullet)$

$$\mathrm{d}\nabla(\bullet) = \nabla\mathrm{d}(\bullet) - \nabla(\bullet)\nabla\mathrm{d}\boldsymbol{u}$$

The 2D discretization is based on a 3-node triangle

$$\boldsymbol{u} = \sum N_K \boldsymbol{u}_K$$

$$\boldsymbol{d} = \sum N_K \boldsymbol{d}_K$$

$$h_z = \sum N_K (h_z)_K$$

We use AceGen for the derivation of the discretized equations

Piezoelectric effect

$E = 69.59$ GPa
$\nu = 0.357$
$\mu = 1.256 \times 10^{-6}$ Hm^{-1}
$\epsilon = 6 \times 10^{-9}$ Fm^{-1}
$\mathscr{I}_{11} = 15.08$ Cm^{-2}
$\mathscr{I}_{12} = -5.207$ Cm^{-2}
$\mathscr{I}_{23} = 12.71$ Cm^{-2}
$\dot{u} = 1$ ms^{-1}

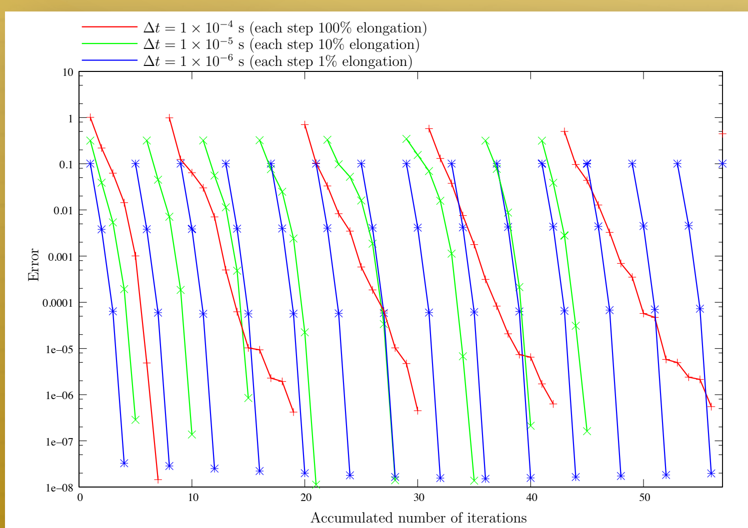

Imposed displacement

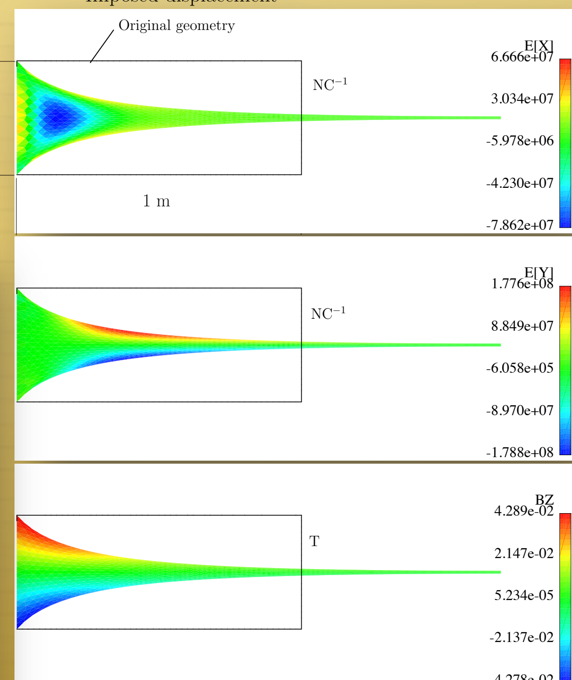

Imposed d_{xx}

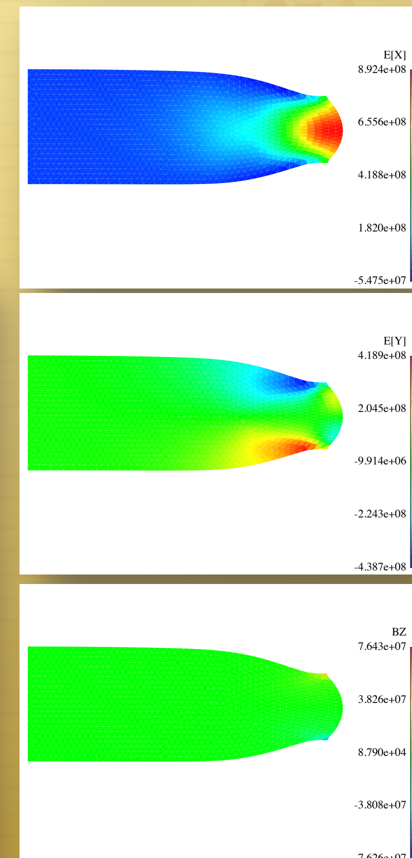

Piezoelectric effect

Damage:

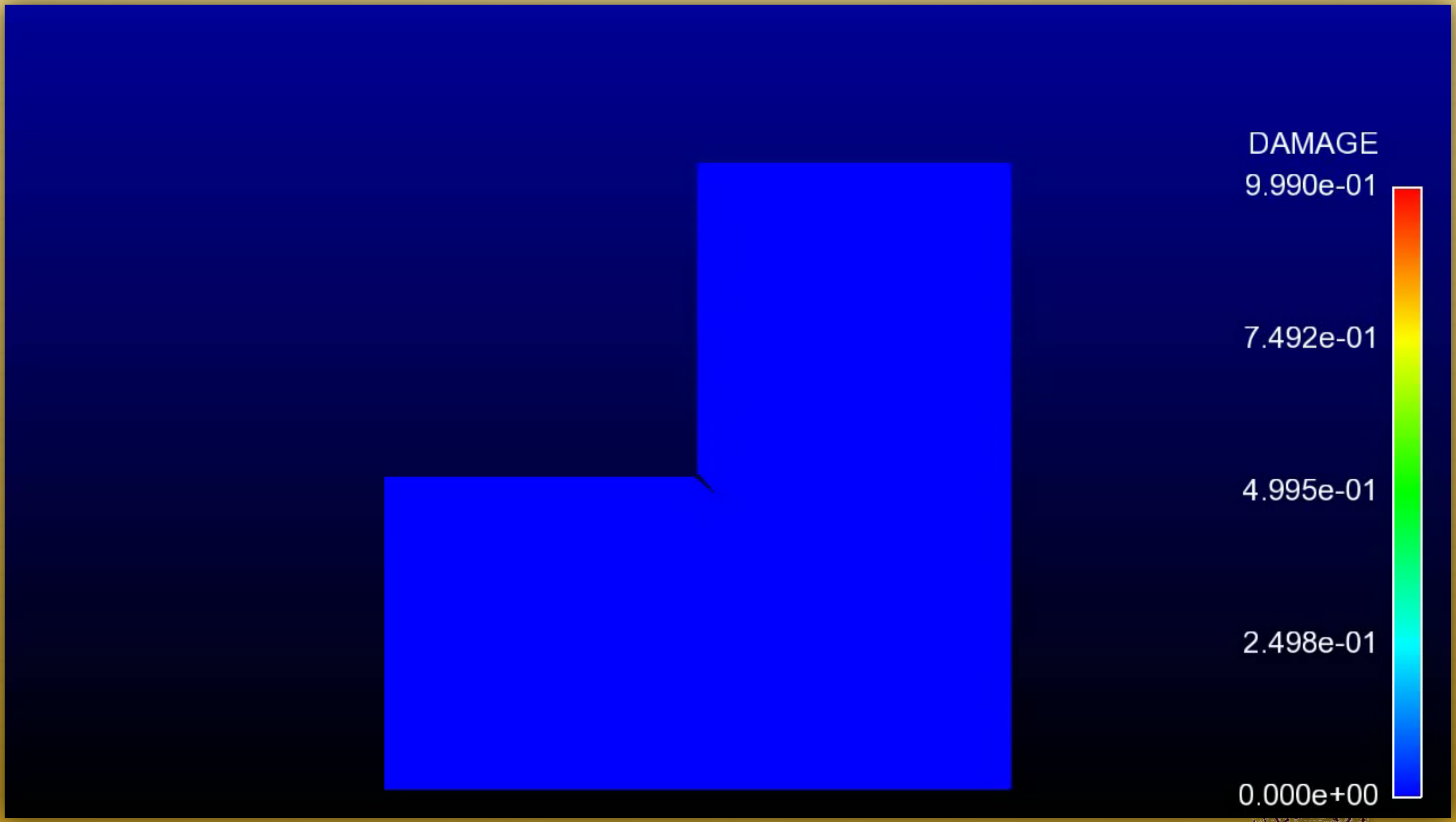

Piezoelectric effect

E_x (V/m):

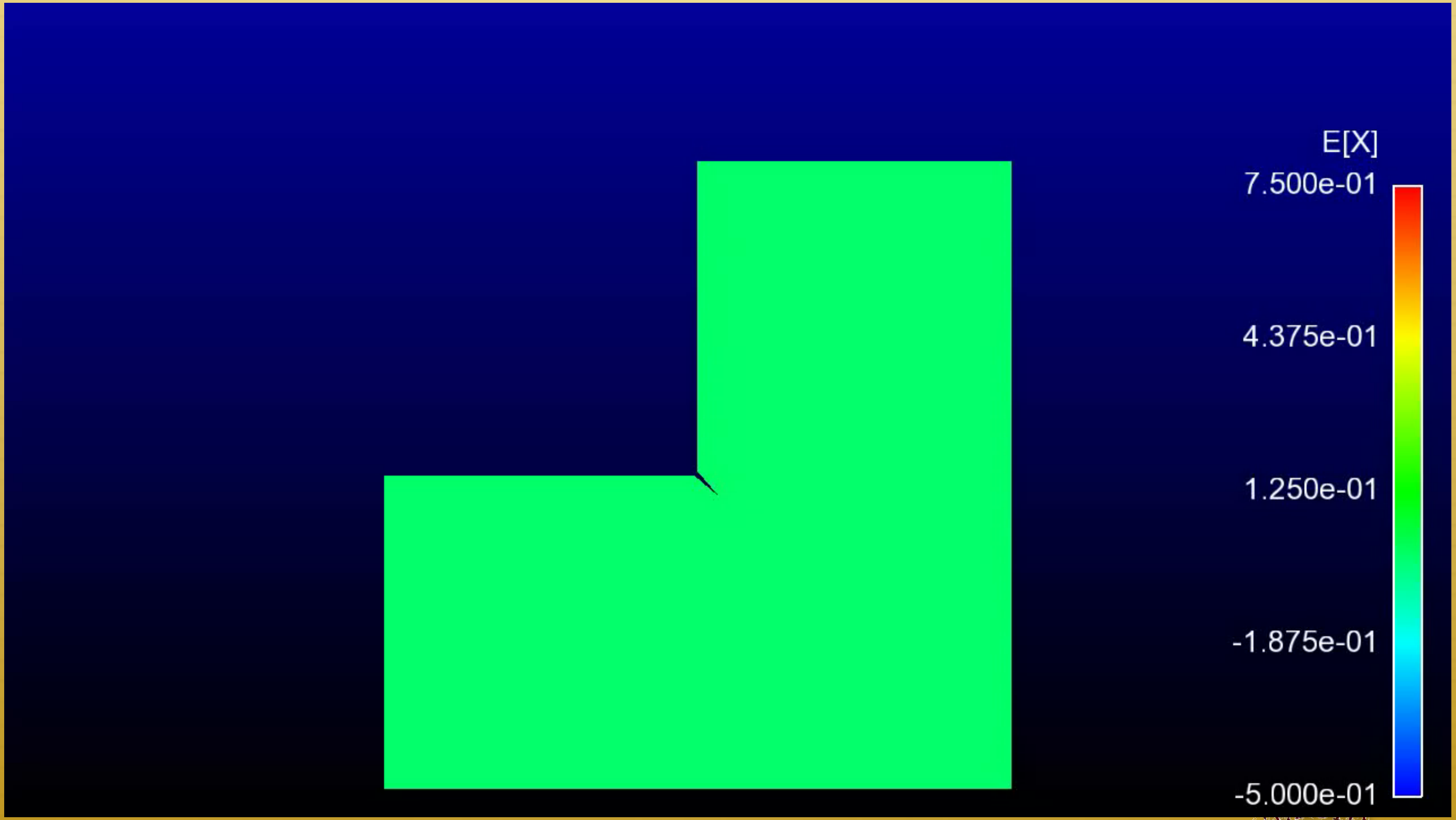

Piezoelectric effect

E_y (V/m):

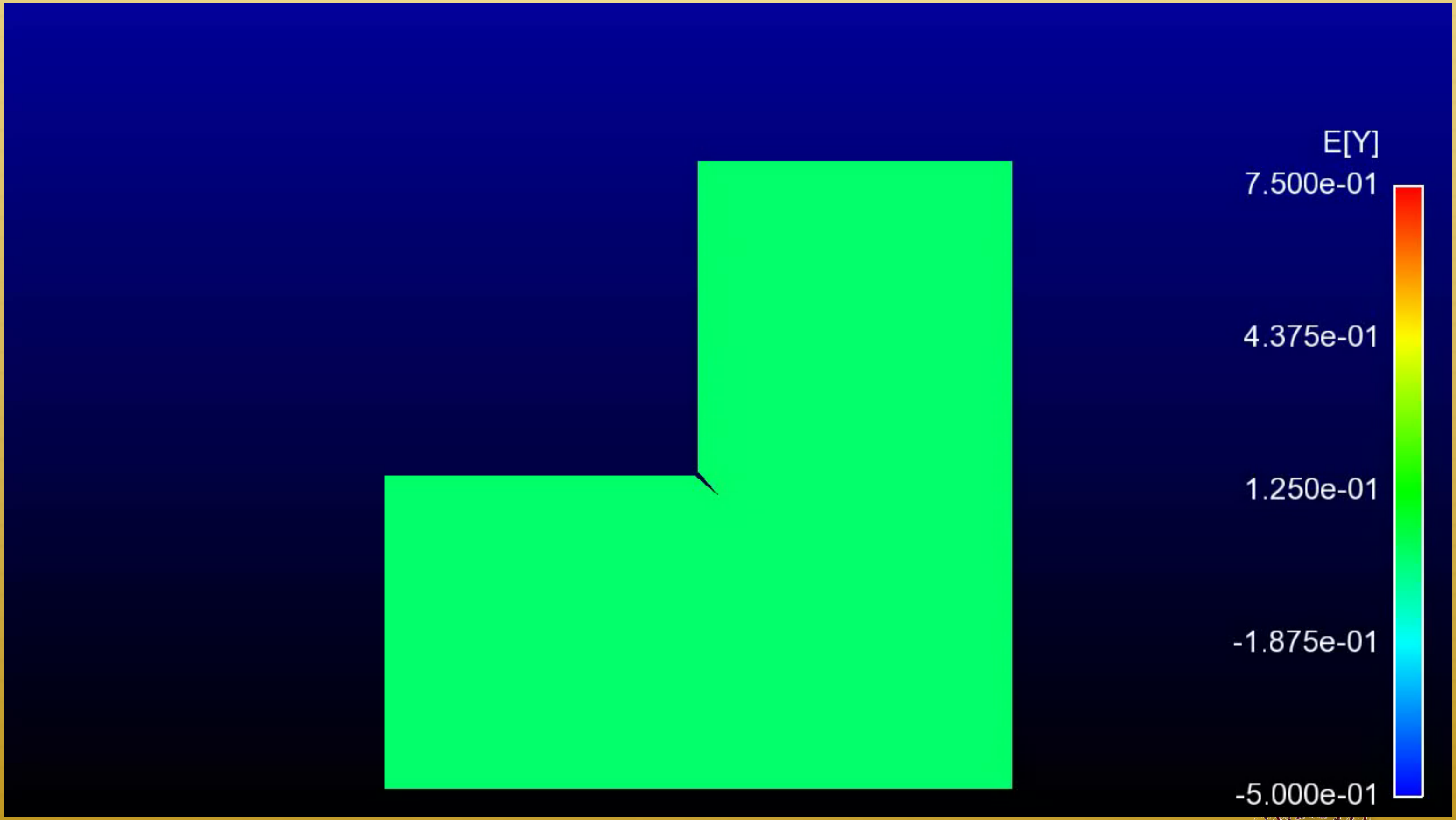

Piezoelectric effect

B_z (T):

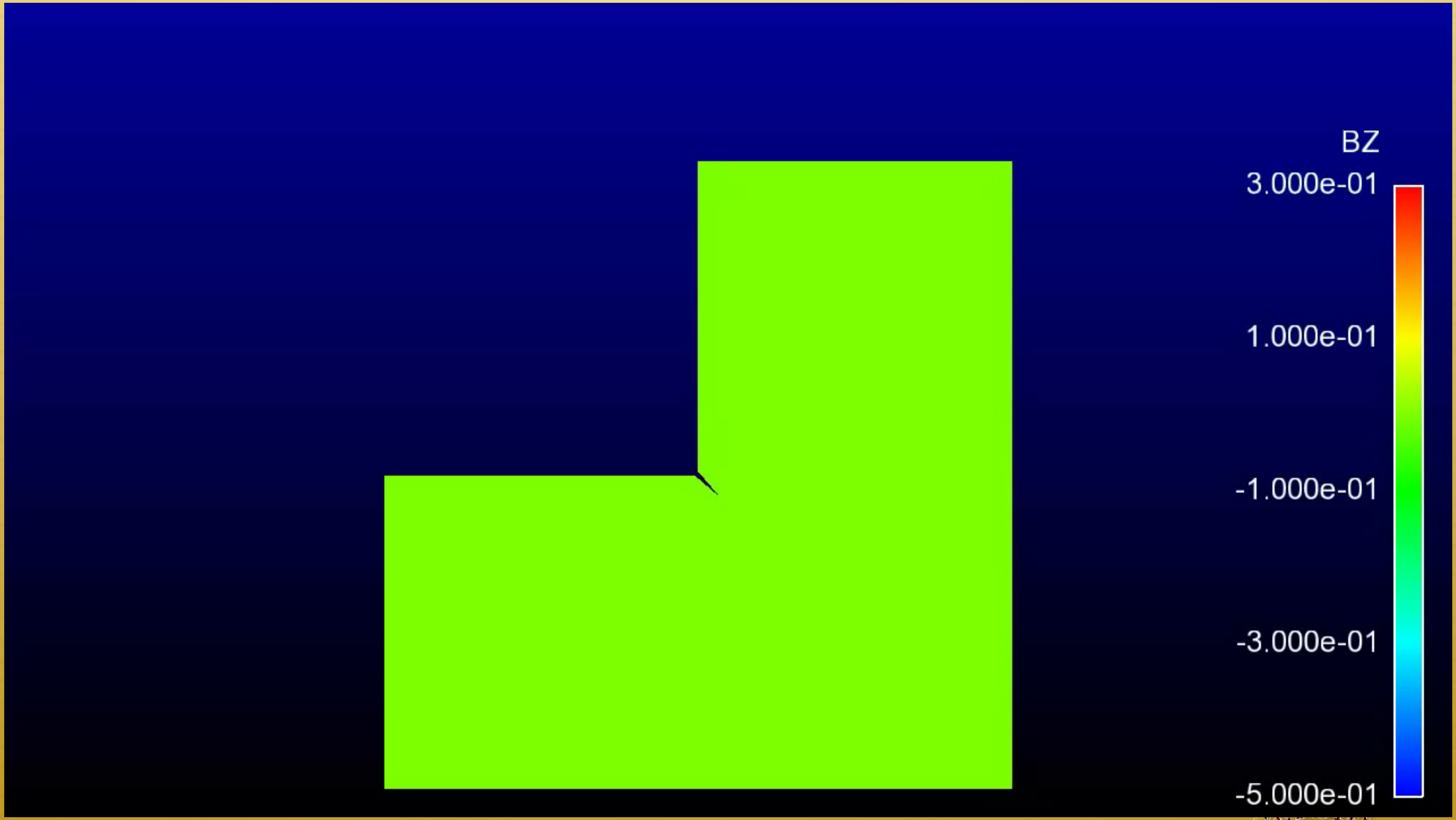

PE: sum-up

- We were able to successfully integrate Cauchy equations of motion and Maxwell equations within a finite strain fracture framework
- Despite oscillations in the magnetic field, we found results physically significant and in agreement with what is expected
- Further verification and validation are required to firmly pursue additions to our approach
- Revision of the boundary conditions and inclusion of anisotropies are natural developments in the theory.

Publications

Publications

- *Seismo-electromagnetic phenomena in the western part of the Eurasia-Nubia plate boundary*, **H.G. Silva**, M. Bezzeghoud, J.P. Rocha, P.F. Biagi, M. Tlemçani, R.N. Rosa, M.A. Salgueiro da Silva, J.F. Borges, B. Caldeira, A.H. Reis, and M. Manso, Nat. Hazards Earth Syst. Sci. 11, 241 (2011).

- *The European VLF/LF radio network to search for earthquake precursors: setting up and natural/man-made disturbances*, P. F. Biagi, T. Maggipinto, F. Righetti, D. Loiacono, L. Schiavulli, T. Ligonzo, A. Ermini, I. A. Moldovan, A. S. Moldovan, A. Buyuksarac, **H.G. Silva**, M. Bezzeghoud, and M. E. Contadakis, Nat. Hazards Earth Syst. Sci. 11, 333 (2011).

- *Atmospheric electrical field anomalies associated with seismic activity*, **H.G. Silva**, M. Bezzeghoud, A.H. Reis, R.N. Rosa, M. Tlemçani, J.F. Borges, B. Caldeira, and P.F. Biagi, Nat. Hazards Earth Syst. Sci. 11, 987 (2011).

- *Analysis of the LF radio signals collected in the European network during about two years*, P. F. Biagi,T. Maggipinto, F. Righetti, L. Schiavulli, T. Ligonzo, A. Ermini, I. A. Moldovan, A. S. Moldovan, A. Buyuksarac, **H.G. Silva**, M. Bezzeghoud, D.N. Arabelos, T.D. Xenos and M. E. Contadakis (submitted).

- *Impedance properties of granitic rocks*, **H.G. Silva**, M.P.F. Graça, J. H. Monteiro, P. Moita, M. Tlemçani, R.N. Rosa, M. Bezzeghoud, S. K. Mendiratta (in preparation).

- *Influence of seismic activity in the atmospheric electrical potential gradient in Lisbon (Portugal) from 1961 until 1991*, **H.G. Silva**, C. Serrano, M.M. Oliveira, M. Bezzeghoud, A.H. Reis, R.N. Rosa, and P.F. Biagi (in preparation).

- *Piezoelectric effect during solid fracture causing electromagnetic emissions*, **H.G. Silva**, P.M. Areias, J.F. Garção, N. Van Goethem, and M. Bezzeghoud (in preparation).

Acknowledgements

Support

ESTÍMULO À CRIATIVIDADE
E À QUALIDADE NA ACTIVIDADE
DE INVESTIGAÇÃO
PROGRAMA DE ESTÍMULO À INVESTIGAÇÃO 2010
FUNDAÇÃO CALOUSTE GULBENKIAN
Serviço de Ciência

Prazo para a entrega das candidaturas: 24 de Setembro de 2010

FUNDAÇÃO CALOUSTE GULBENKIAN

QREN
QUADRO
DE REFERÊNCIA
ESTRATÉGICO
NACIONAL
PORTUGAL 2007.2013

adi
agência de inovação

FCT Fundação para a Ciência e a Tecnologia
MINISTÉRIO DA CIÊNCIA, TECNOLOGIA E ENSINO SUPERIOR

Collaborations

i3N
INSTITUTE FOR NANOSTRUCTURES, NANOMODELLING AND NANOFABRICATION
RESEARCH, INNOVATION AND ENGINEERING APPLICATIONS

UNIVERSITÀ DEGLI STUDI DI BARI ALDO MORO

U. PORTO

Thank you very much
for your attention!

UNIVERSIDADE DE EVORA
CGE